

Experimental Study of a 33.3-GHz Free-Electron-Laser Amplifier with a Reversed Axial Guide Magnetic Field

M. E. Conde and G. Bekefi

Department of Physics and Research Laboratory of Electronics, Massachusetts Institute of Technology, Cambridge, Massachusetts 02139

(Received 22 July 1991)

We report on a new regime of free-electron-laser operation with reversed axial guide magnetic field, in which the rotational motion of the electrons in the helical wiggler field is opposed by the presence of the uniform guide field. The 33.3-GHz free-electron-laser amplifier is driven by a mildly relativistic electron beam (750 kV, 300 A, 30 ns) and generates 61 MW of radiation with a 27% conversion efficiency. Measurements with the conventional orientation of the axial field show a considerable loss of power and efficiency.

PACS numbers: 42.55.Tb

The free-electron laser (FEL) operating in a combined axial guide magnetic field and a helical wiggler field has been studied experimentally [1,2] and theoretically [3] over a period of many years, in both linear and nonlinear regimes. In all these studies, the axial magnetic field B_z is oriented so that the cyclotron rotation of the beam electrons is in the same direction as the rotation imposed by the helical wiggler field B_w . This leads to an increase [4-6] of the transverse electron velocity v_\perp compared to what it would be in the absence of B_z , with potential benefits such as an enhanced radiation growth rate and efficiency [3]. Indeed, when the cyclotron wavelength in the axial field $\lambda_c = 2\pi v_z / \Omega_z$ approaches the wiggler periodicity l_w the transverse electron excursions can become too large, the electrons strike the drift tube wall and are lost ($\Omega_z = eB_z / m_0 \gamma$ is the cyclotron frequency in the guide field and $\gamma = [1 - (v_z/c)^2 - (v_\perp/c)^2]^{-1/2}$ is the relativistic energy factor). Thus, the "resonance" $\lambda_c = l_w$ becomes a dividing line for conventional FEL operation: At relatively weak axial fields, $\lambda_c > l_w$, we have the so-called group-I regime, and for stronger fields such that $\lambda_c < l_w$, the group-II regime.

In this Letter we report measurements using a new, hitherto unexplored configuration with a reversed axial magnetic field. The rotation of the electrons in the helical wiggler field B_w is now opposed by the presence of the guide field B_z and there is no longer the resonance at $\lambda_c = l_w$. The transverse electron velocity v_\perp is diminished compared to what it would be in the absence of B_z (however, the latter reduction is partially compensated in our experiments by increasing B_w). We will show that a reversal of B_z yields higher radiation intensity and efficiency compared to what we were able to achieve with the conventional orientation of the axial magnetic field.

The three regimes of FEL operation (group I, group II, and reversed field) are displayed in Fig. 1 based on a particle trajectory calculation of v_z/c which neglects space charge and radiation, and assumes that the electrons are undergoing ideal helical orbits in the combined B_z and B_w fields. The solid points illustrate the three parameter re-

gimes of B_z where maximum radiation has been observed in our experiments.

A schematic of the FEL amplifier is shown in Fig. 2. A mildly relativistic electron beam (750 ± 50 keV) is generated by a Marx capacitor bank (Physics International Pulserad 110 A). The electrons are emitted from a hemispherical graphite cathode by an explosive field-emission process. The graphite anode acts as an emittance selector, allowing only a small fraction of the current to propagate through its 2.54-mm radius and 62-mm-long aperture. The electron beam current downstream from the emittance selector, and in the absence of the wiggler field, is illustrated in Fig. 3(a), showing saturation at high B_z where all available electrons from the gun have made it through the anode hole. Using the technique of Ref. [7] we estimate the normalized rms beam emittance to be $\epsilon_n < 4.4 \times 10^{-2}$ cm rad and the corresponding rms axial energy spread to be $\Delta\gamma_z/\gamma_z < 1.5 \times 10^{-2}$. We observe from Fig. 3(b) that when the wiggler is turned on, an expected very pronounced cur-

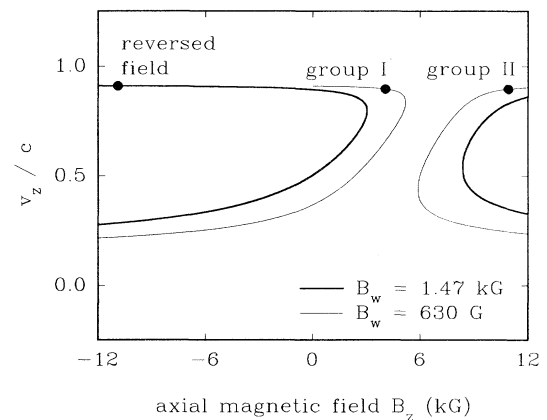


FIG. 1. Ideal equilibrium electron orbits calculated for two different values of wiggler magnetic field. The solid points show the values of B_z where maximum power is observed for group-I, group-II, and reversed-field regimes.

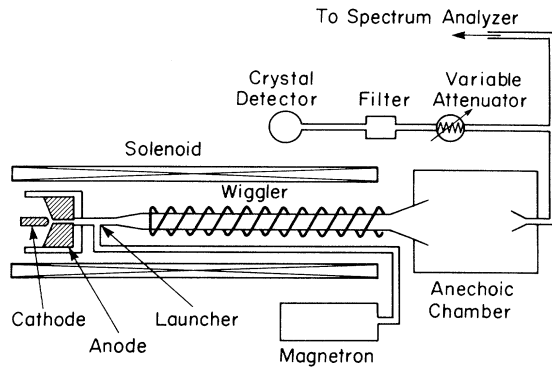


FIG. 2. Free-electron-laser experimental setup.

rent loss occurs near resonance $\lambda_c = l_w$ with the conventional orientation of B_z . This happens because the transverse velocity of the electrons becomes too large and eventually they are lost to the waveguide walls. No significant current loss (also as expected) is seen with the magnetic field reversed [Fig. 3(c)].

The 50-period bifilar helical wiggler produced by current-carrying helical wires has a period of 3.18 cm and provides a magnetic field whose magnitude on axis is adjustable up to 1.8 kG. The wiggler field intensity is slowly increased over the initial six periods, providing an adiabatic input for the electron beam. The system, including the gun, is immersed in a uniform axial magnetic field generated by a solenoid. The intensity of this field can be varied up to a maximum of 11.6 kG.

The 2-m-long stainless-steel drift tube has an internal radius of 0.51 cm and acts as a cylindrical waveguide whose fundamental TE_{11} mode has a cutoff frequency of 17.2 GHz. The system is designed to operate in this lowest waveguide mode.

A high-power magnetron operating at 33.39 GHz is the input power source for the FEL amplifier. The wave launcher consists of a short section of circular waveguide of radius 0.31 cm into which 17 kW are coupled from a standard Ka-band rectangular waveguide. This section of circular waveguide supports only the fundamental TE_{11} mode for the operating frequency. Its radius is then adiabatically increased to the radius of the drift tube. A linearly polarized wave is thereby injected into the interaction region. Half of the incident power, with the correct rotation of the electric-field vector, participates in the FEL interaction.

The output power from the FEL is transmitted by means of a conical horn into a reflection free "anechoic chamber." A small fraction of the radiation is then collected by a receiving horn, passes through precision calibrated attenuators, and a 1.7-GHz-wide band-pass filter. The power level is finally determined from the response of a calibrated crystal detector. The entire system is calibrated by a substitution method, i.e., by turning off the electron beam and measuring the received power relative to the magnetron power. This technique avoids calibra-

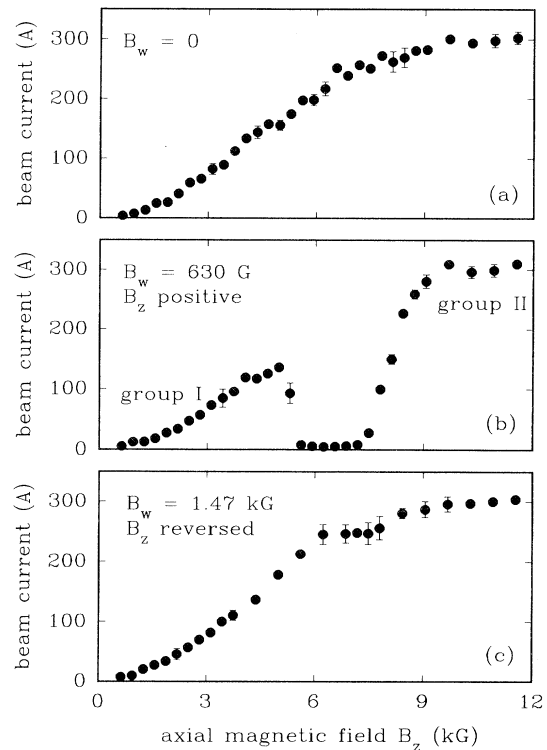


FIG. 3. Electron beam current in the FEL as a function of the axial guide magnetic field B_z : (a) no wiggler magnetic field; (b) wiggler field $B_w = 630$ G and B_z in the conventional direction; (c) wiggler field $B_w = 1.47$ kG and B_z in the reversed direction.

tion uncertainties due to things like waveguide attenuation (~ 1 dB/m).

Angular scans of the radiation pattern of the transmitting horn carried out within the anechoic chamber together with a set of high-pass waveguide filters are used to confirm that the FEL indeed operates in the TE_{11} waveguide mode. The frequency spectrum of the output power has also been determined by a heterodyne technique (see Fig. 2). A crystal rectifier is used as a mixer for the 33-GHz FEL radiation and for radiation from a variable-frequency 23-GHz local oscillator. The beat wave is amplified by a TWT amplifier and sent into a filter bank, composed of thirteen channels adjacent in frequency, each 80 MHz wide. Thus, on a single-shot basis, the radiation frequency is determined to be 33.39 GHz with a full width at half maximum of less than 160 MHz.

A parameter scan of the output power has been carried out in order to discover the optimum operating conditions for our three regimes, group I, group II, and reversed field. Figure 4(a) illustrates the output power as a function of B_w at constant B_z , and Figs. 4(b) and 4(c) show how the power varies with B_z at constant B_w . It is seen that the maximum output power obtained in the group-I and group-II regimes is approximately the same, 5 MW; however, the efficiency is much higher for the group-I re-

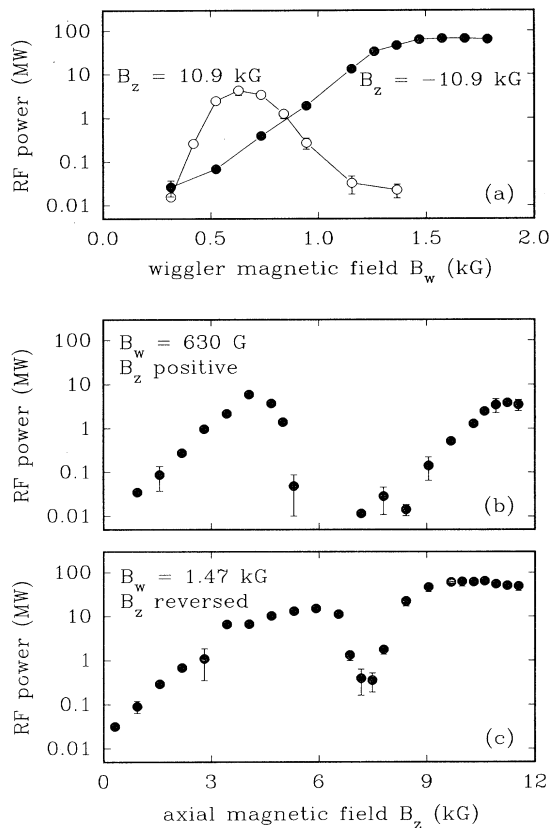


FIG. 4. FEL output power as a function of B_z and B_w : (a) B_w scan for fixed $B_z = 10.9$ kG in each direction; (b) B_z scan in the conventional direction for fixed $B_w = 630$ G; (c) B_z scan in the reversed direction for fixed $B_w = 1.47$ kG.

gime since here the beam current is smaller. The output power for the reversed-field case is higher by an order of magnitude and reaches a level of 61 MW.

The spatial growth of the electromagnetic wave intensity is determined from the measurement of the output power as a function of the length of the interaction region. This length is varied by changing the distance that the electron beam is allowed to propagate in the drift tube. Application of a strong magnetic field is sufficient to deflect the electrons into the waveguide wall and thereby terminate the interaction at that point. Figure 5 shows the result of this measurement for the three different regimes. In the group-I regime the power level reaches saturation at 5.8 MW corresponding to an efficiency of 9%. Operation in group II shows the lowest efficiency (2%). The reversed-field operation has by far the highest efficiency (27%), and exhibits no power saturation (Table I).

In conclusion, we have found that our free-electron laser shows highest efficiency and highest power output when operated with reversed axial guide magnetic field. Table I summarizes our findings. We believe that the 27% efficiency of our system exceeds the efficiency of pre-

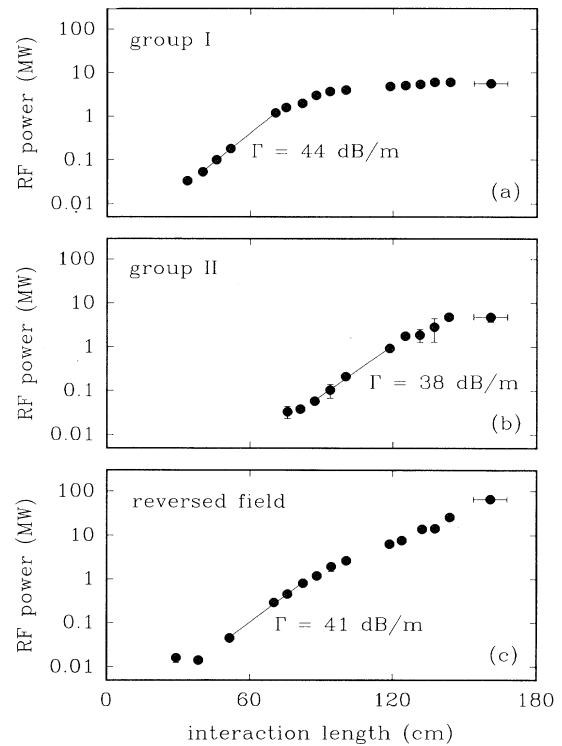


FIG. 5. FEL output power as a function of interaction length: (a) group-I regime; (b) group-II regime; (c) reversed-field regime. The Γ 's represent growth rate estimates over interaction regions indicated by the straight lines.

vious FELs with untapered wigglers. If the ~ 1 -dB/m attenuation due to the stainless-steel waveguide were subtracted from the measurements, the power and efficiency could be substantially higher. Moreover, Fig. 5(c) shows that our wiggler is too short to reach saturation, and much higher efficiency may well be possible with longer and/or tapered magnetic fields.

We note that our FEL falls into the so-called Raman parameter regime where *reversed-field* space-charge effects must be allowed for, in order to account for both the radiation frequency and the power output. A detailed theoretical understanding of the reversed-field FEL is as yet unavailable due in part to some lack of understanding

TABLE I. Summary of experimental results.

Parameter	Group I	Group II	Reversed field
Frequency (GHz)	33.39	33.39	33.39
Beam energy (keV)	750	750	750
Beam current (A)	90	300	300
Guide field (kG)	4.06	10.9	-10.9
Wiggler field (kG)	0.63	0.63	1.47
Output power (MW)	5.8	4.2	61
Efficiency (%)	9	2	27

of the electron trajectories themselves. This is clearly shown in Fig. 4(c), where a large, unexpected dip in output power occurs near $l_w \approx -\lambda_c$ ($B_z \approx -7.6$ kG), but no such dip occurs either in the electron current [Fig. 3(c)] or in calculations based on ideal orbit theory. Thus, the ideal orbit model on which Fig. 1 is based may well need substantial modification when B_z is reversed from its usual orientation.

This study was supported by DOE, AFOSR, and CNPq (Brazil). We thank I. Mastovsky, C. J. Taylor, and T. Mizuno for the assistance in the experimental work.

Note added.—After submission of this work, perturbation analyses [8,9] of the particle motion in the reversed-field configuration do indeed indicate departures from the ideal orbit model near $l_w \approx -\lambda_c$. This effect is attributed to electrons with off-axis guiding centers, and is the result of betatronlike oscillations. The departure from the ideal orbits causes a decrease in v_z , detuning of the FEL, and a

subsequent intensity degradation.

- [1] S. H. Gold, D. L. Hardesty, A. K. Kinkead, L. R. Barnett, and V. L. Granatstein, Phys. Rev. Lett. **52**, 1218 (1984).
- [2] J. Fajans, J. S. Wurtele, G. Bekefi, D. S. Knowles, and K. Xu, Phys. Rev. Lett. **57**, 579 (1986); also, J. Fajans, G. Bekefi, Y. Z. Yin, and B. Lax, Phys. Fluids **28**, 1995 (1985).
- [3] A. K. Ganguly and H. P. Freund, IEEE Trans. Plasma Sci. **16**, 167 (1988).
- [4] L. Friedland, Phys. Fluids **23**, 2376 (1980).
- [5] P. Diament, Phys. Rev. A **23**, 2537 (1981).
- [6] H. P. Freund and A. K. Ganguly, IEEE J. Quantum Electron. **21**, 1073 (1985).
- [7] D. Prosnitz and E. T. Scharlemann, LLNL ATA Note No. 229, 1984.
- [8] K. R. Chu and A. T. Lin, University of California, Los Angeles, Report No. PPG-1373, 1991 (to be published).
- [9] G. Shvets and J. S. Wurtele (private communication).